



Published in final edited form as:

Vascul Pharmacol. 2023 December ; 153: 107246. doi:10.1016/j.vph.2023.107246.

Activated CTHRC1 Promotes Glycolysis in Endothelial Cells: Implications for Metabolism and Angiogenesis

Barbara H. Toomey^a, Sarah-A. Mitrovic^b, Maia Lindner-Liaw^a, Ruth G. Leon Vazquez^c, Victoria E. DeMambro^a, Doreen Kacer^a, Sergey Ryzhov^a, Igor Prudovsky^a, Volkhard Lindner, M.D., Ph.D.^{a,*}

^aCenter for Molecular Medicine, MaineHealth Institute for Research, 81 Research Drive, Scarborough, ME 04074, United States

^bBoehringer Ingelheim Pharma GmbH & KG, Medicinal Chemistry, Birkendorfer Str.65, 88400 Biberach, Germany

^cDepartment of Biochemistry, University of Puerto Rico, School of Medicine, San Juan, Puerto Rico, 00936-5067

Abstract

CTHRC1 is transiently expressed by activated fibroblasts during tissue repair and in certain cancers, and CTHRC1 derived from osteocytes is detectable in circulation. Because its biological

*Corresponding Author Volkhard Lindner, M.D., Ph.D., MaineHealth Institute for Research, 81 Research Drive, Scarborough, ME 04074, Phone: 207-396-8143, Fax: 207-396-8179, volkhard.lindner@mainehealth.org.

Author Statement

Conceptualization; Data curation; Formal analysis; Funding acquisition; Investigation; Methodology; Project administration; Resources; Software; Supervision; Validation; Visualization; Roles/Writing - original draft; Writing - review & editing. Authorship statements should be formatted with the names of authors first and CRediT role(s) following.

1. Barbara Toomey: Conceptualization; Data curation; Formal analysis; Investigation; Methodology; Visualization; Roles/Writing - original draft; Writing - review & editing
2. Sarah-A. Mitrovic: Data curation; Formal analysis; Methodology; Investigation; Writing - review & editing
3. Maia Lindner-Liaw: Formal analysis; Software; Roles/Writing - original draft
4. Ruth Leon Vasquez: Data curation; Formal analysis
5. Victoria E. DeMambro: Seahorse data curation, formal analysis
6. Doreen Kacer: Data curation; Formal analysis; Methodology
7. Sergey Ryzhov: Funding acquisition; Writing - review & editing
8. Igor Prudovsky: Conceptualization; Data curation; Formal analysis; Investigation; Methodology; Visualization; Roles/Writing - original draft; Writing - review & editing
9. Volkhard Lindner: Conceptualization; Data curation; Formal analysis; Funding acquisition; Investigation; Methodology; Project administration; Resources; Supervision; Validation; Visualization; Roles/Writing - original draft; Writing - review & editing

Declaration of interests

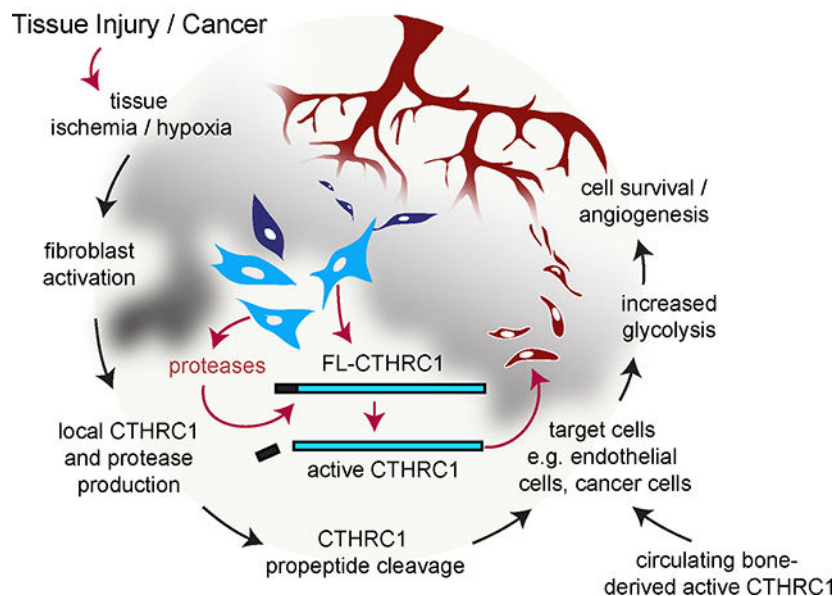
The authors declare that they have no known competing financial interests or personal relationships that could have appeared to influence the work reported in this paper.

Disclosures: The authors have no conflicts to disclose.

Publisher's Disclaimer: This is a PDF file of an unedited manuscript that has been accepted for publication. As a service to our customers we are providing this early version of the manuscript. The manuscript will undergo copyediting, typesetting, and review of the resulting proof before it is published in its final form. Please note that during the production process errors may be discovered which could affect the content, and all legal disclaimers that apply to the journal pertain.

activity is poorly understood, we investigated whether the N terminus of CTHRC1 encodes a propeptide requiring cleavage to become activated. The effects of full-length versus cleaved recombinant CTHRC1 on endothelial cell metabolism and gene expression were examined *in vitro*. Respirometry was performed on *Cthrc1* null and wildtype mice to obtain evidence for biological activity of CTHRC1 *in vivo*. Cleavage of the propeptide observed *in vitro* was attenuated in the presence of protease inhibitors, and cleaved CTHRC1 significantly promoted glycolysis whereas full-length CTHRC1 was less effective. The respiratory exchange ratio was significantly higher in wildtype mice compared to *Cthrc1* null mice, supporting the findings of CTHRC1 promoting glycolysis *in vivo*. Key enzymes involved in glycolysis were significantly upregulated in endothelial cells in response to treatment with CTHRC1. In healthy human subjects, 58% of the cohort had detectable levels of circulating full-length CTHRC1, whereas all subjects with undetectable levels of full-length CTHRC1 (with one exception) had measurable levels of truncated CTHRC1 (88 pg/ml to >400 ng/ml). Our findings support a concept where CTHRC1 induction in activated fibroblasts at sites of ischemia such as tissue injury or cancer functions to increase glycolysis for ATP production under hypoxic conditions, thereby promoting cell survival and tissue repair. By promoting glycolysis under normoxic conditions, CTHRC1 may also be a contributor to the Warburg effect characteristically observed in many cancers.

Graphical Abstract



Keywords

CTHRC1; propeptide; metabolism; glycolysis; respiratory exchange ratio; Warburg effect

1. Introduction

CTHRC1, collagen triple helix repeat containing 1, is a secreted protein transiently expressed during tissue repair and remodeling¹ such as after arterial injury where we first identified it², after myocardial infarction³ and during remodeling of cancer stroma

⁴. While expression of CTHRC1 is not detectable in normal arteries or the healthy heart, it is prominently induced in a subset of activated fibroblasts within three days of injury, followed by a decline in expression over the course of a few weeks. Constitutive expression of CTHRC1 occurs in bone by osteocytes and osteoblasts from where it is released into circulation ^{4,5}. It is also constitutively expressed by some neurons in certain regions of the brain ⁶. Disruption of the *Cthrc1* gene in mice leads to phenotypic changes indicative of metabolic function ¹, including reductions in trabecular bone mass ⁵, increased body fat, reduced muscle mass as well as reduced physical activity ⁶. We and others have also demonstrated that the fibroblast-like synoviocyte characteristic of inflammatory arthritis expresses high levels of CTHRC1 ^{5,7,8}. Myngbay et al. ⁷ further reported that rheumatoid arthritis was associated with increased CTHRC1 plasma levels.

The short collagen domain of twelve G-X-Y repeats within CTHRC1 enables the protein to form trimers ². We previously reported that CTHRC1 present in the culture medium of a smooth muscle cell line transduced with a *Cthrc1* expression vector had a lower molecular weight than CTHRC1 in the cytoplasm as a result of N terminal truncation ⁹ due to cleavage after the amino acid residue E46 of human CTHRC1 (E48 of rat/mouse CTHRC1). The significance and mechanism of this cleavage event has hitherto remained insufficiently characterized. The present study therefore sought to address whether the N terminal fragment of predominantly basic amino acids represents a propeptide that requires cleavage for CTHRC1 to become biologically active. Furthermore, we sought to identify the factors mediating cleavage, and we assessed the plasma levels of full-length and N terminally truncated CTHRC1 in a cohort of healthy human subjects to gain insight into the prevalence of these two forms of CTHRC1 *in vivo*. Finally, we identified a role for CTHRC1 in cellular metabolism allowing us to explain its biological effects.

2. Materials and Methods

2.1. Monoclonal antibody generation and ELISA development

The coding region of hFL-CTHRC1 without the signal peptide was cloned in frame with the N terminal 6xHis into the pEQ30 vector (Qiagen) for expression in *E.Coli*. hFL-CTHRC1 protein purified with Ni-NTA Agarose (Qiagen) was used for immunization of *Cthrc1* null mice ¹. Additional mice were immunized with synthetic peptides (New England Peptide, Gardner, MA) of the human (aa31–46), SEIPKGGKQKAQLRQRE) or the rat/mouse (aa33–48, SENPKGGKQKALIRQRE) N terminal sequence conjugated to keyhole limpet hemocyanin (KLH)⁴. Rabbits were immunized with a synthetic peptide of the conserved sequence following the propeptide (aa47–62, VVDLYNGMCLQGPAGV), also conjugated to KLH.

Vli13E09 was used at a concentration of 1–2µg/ml in carbonate buffer (50mM, pH9.6) as the capturing antibody for coating ELISA strip wells (Thermo Scientific, Nunc, MaxiSorp, flat bottom) for 14h at 4°C. Protein A/G purified IgGs of Vli10G07, Vli08G09 and Vli42 were conjugated with biotin using EZ-Link Sulfo-NHS-LC-LC-Biotin (Thermo Scientific), following the manufacturer's instructions. Additional details about the ELISA are in the supplemental data file.

2.2. Analysis of cell metabolism

All metabolic assays were performed on HUVECs using an Agilent Seahorse XF96 Analyzer. HUVECs were plated at 5000 cells per well in the Seahorse TC96 analytical plates under four types of media: 1. Control medium. It contained ¼ volume of conditioned medium from beta-galactosidase transduced 3T3-L1 cells; 2. Recombinant hFL-CTHRC1 (200ng/ml) in control medium; 3. Recombinant VVD-CTHRC1 (200ng/ml) in control medium; 4. Medium containing ¼ volume of conditioned medium from hFL-CTHRC1 transduced 3T3-L1 cells. Additional details are in the supplemental data file.

2.3. Ethics statement

All protocols involving animals were approved by the Institutional Animal Care and Use Committee of the Maine Medical Center (protocol number 2105) and were in compliance with all applicable regulations and guidelines including the National Institutes of Health Guide for Care and Use of Laboratory Animals. *Cthrc1* null mice with global inactivation of the *Cthrc1* gene have been previously described¹.

Human plasma samples were from a previously reported study⁴. Human plasma samples were obtained under a protocol approved by the Institutional Review Board (IRB) of Maine Medical Center (protocol number 3657). EDTA plasma samples were obtained from healthy adult male and female volunteers after obtaining written informed consent (male and female, 20–65 years of age). The IRB had approved the Informed Consent Form (ICF) and the procedure used to consent participants for the blood draw. After consenting, the participants were provided with a signed copy of the ICF. The original signed copy of the ICF is kept by the investigators in a secure place.

2.4. Mouse respiratory exchange ratio (RER)

studies are described in detail in the supplemental data file.

2.5. Statistical analyses of CTHRC1 plasma levels

Statistical analyses were conducted in the R programming language. Maximum likelihood methods were used to obtain parameter estimates for the data, and distributions were assessed using the Pearson Goodness-of-Fit Test. CTHRC1 levels were set to zero if below the detection limit and the one sample exceeding 400ng/ml was set to 400ng/ml.

3. Results

3.1 Recognition of CTHRC1 epitopes by monoclonal antibodies

Hybridoma cell lines expressing mouse monoclonal IgG1-kappa specific for the hCTHRC1 propeptide (clone Vli10G07), specific for the mouse/rat propeptide (clone Vli08G09), and a rabbit monoclonal IgG specific for the conserved sequence following the propeptide (clone Vli42) were obtained (https://mhir.org/?page_id=2008). In addition, a mouse monoclonal IgG1kappa recognizing a conserved internal epitope located between aa62 and aa243 (clone Vli13E09) was obtained as well⁴. A schematic of the epitopes recognized by the antibodies is shown in Fig. 1.

Detailed characterization of the monoclonal antibodies is provided on the website (https://mhir.org/?page_id=2008). All CTHRC1 antibodies were verified on knockout mouse tissues and mice overexpressing transgenic CTHRC1 heterotopically. The peptide affinity purified polyclonal IgG against aa47–62 (VVDLYNGMCLQGPAV) that gave rise to clone Vli42 had a $K_d=7\text{nM}$ for cleaved CTHRC1 and a $K_d=70\text{nM}$ for hFL-CTHRC1 as determined by surface plasmon resonance (SPR). For Vli13E09 the $K_d=20\text{nM}$ for FL-CTHRC1 was established by SPR.

3.2 Full-length and cleaved CTHRC1 levels in conditioned media from transfected cells

Following transfection with hFL-CTHRC1 expression constructs, levels of hFL-CTHRC1 protein secreted from cells into the medium were monitored over time by ELISA (Fig. 2), with or without serum present in the culture medium. The use of Vli10G07 in the ELISA allowed for specific detection of hFL-CTHRC1 in the medium, whereas using Vli42 in the ELISA detected both hFL-CTHRC1 as well as N terminally truncated VVD-CTHRC1.

The amount of CTHRC1 detectable in the medium will depend on the kinetics of expression and secretion from the cells, and on the half-life of CTHRC1 in the medium. When CHOK1 and HEK293T cells were transfected with the hFL-CTHRC1 construct and incubated in the absence of serum, much less cleavage of the N terminal fragment occurred compared to incubation of the same cells in the presence of 10% serum (Fig. 2). In the presence of serum, the highest levels of hFL-CTHRC1 were seen at 24 hours after transfection with a steady decrease over the following three days (Fig. 2A, B). However, total CTHRC1 (hFL-CTHRC1 and VVD-CTHRC1 as detected with the Vli42 ELISA) remained at similar levels between 24 and 96 hours after transfection (Fig. 2A, B). Of note, the optical density readings in the Vli42 ELISA are lower than the Vli10G07 ELISA, indicating higher sensitivity of the ELISA detecting only hFL-CTHRC1. In the absence of serum, hFL-CTHRC1 remained at similar levels between 24 and 96 hours after transfection, suggesting that the presence of serum was associated with N terminal cleavage of CTHRC1. These findings were supported by Western blotting demonstrating the presence of a CTHRC1 double band in the medium containing serum, with the lower band increasing in intensity over time. Only the upper band of CTHRC1 was seen under serum free conditions (Fig. 2C). In addition, the 24-hour time point demonstrates that detection of CTHRC1 by ELISA is more sensitive with a wider dynamic range than detection by Western blotting.

To provide further proof that the N terminus of CTHRC1 is sensitive to cleavage we transfected HEK293T cells with an hFL-CTHRC1 expression construct encoding a 7xHis tag fused to the N terminus. This allowed for better visualization of the cleavage by Western blotting due to the increased molecular mass of the cleaved N terminal fragment, thereby increasing the difference in molecular weight between cleaved and uncleaved CTHRC1. Western blotting for CTHRC1 with Vli10G07 specific for the propeptide and with Vli13E09 recognizing an internal epitope are shown in Fig. 2D. The propeptide epitope is not detectable in the medium of cells expressing CTHRC1 in the presence of serum. A much less prominent and sharp band of slightly lower molecular mass detected by Vli10G07 likely reflects under-glycosylated CTHRC1 (Fig. 2D). Specificity of Vli10G07 for the propeptide is further demonstrated by the inability to detect N terminally truncated VVD-CTHRC1.

Western blotting with rabbit monoclonal antibody Vli55 recognizing the C terminus of CTHRC1 showed similar results as Vli13E09 (data not shown).

3.3. Cleavage of exogenous CTHRC1 added to cells

The studies above examined cleavage of CTHRC1 in transfected cells where expression and secretion of CTHRC1 from cells is ongoing simultaneously with propeptide cleavage. To clarify further that propeptide cleavage occurs extracellularly, we added media containing hFL-CTHRC1 to cells and monitored cleavage of the N terminus by ELISA. Adding it to HEK293T cells caused most of the full-length CTHRC1 to be cleaved within 24 hours (Fig. 3A).

Interestingly, propeptide cleavage occurred not only in cells growing in the presence of serum but also in cells growing in the absence of serum (Fig. 3A). A protease inhibitor cocktail partially inhibited cleavage under serum free conditions in this experiment. The accelerated propeptide cleavage in this experiment can at least in part be explained by the absence of ongoing CTHRC1 expression by the cells. Experiments with other cell types including pulmonary artery smooth muscle (PAC-1)⁹, mouse cardiac endothelial cells (MCEC-1, ATCC), and RAW264.7 cells (ATCC) showed a similar pattern of a rapid decline in hFL-CTHRC1 levels when added to the cells (data not shown).

To determine if intracellular factors released from damaged cells were involved in CTHRC1 cleavage, we incubated hFL-CTHRC1 CM in the presence of cell lysate from HEK293T cells under serum free conditions. We found that added cell lysate promoted propeptide cleavage which was inhibited by a cocktail of protease inhibitors (Fig. 3B). Cleavage by individual inhibitors present in the cocktail had little effect (data not shown). A similar experiment with transfected cells overexpressing hFL-CTHRC1 also showed increased propeptide cleavage in the presence of added cell lysate under serum free conditions (data not shown). These data suggest that an intracellular protease might be contributing to propeptide cleavage.

Different from previously reported results, the plasmin inhibitor ϵ -aminocaproic acid failed to reduce propeptide cleavage (Fig. 3C). Online tools predicting protease cleavage sites (ExPasy, peptide cutter) indicated that cleavage between E46 and V47 could be mediated by glutamylendopeptidase (ENPEP, also known as aminopeptidase A), however, the ENPEP inhibitor Amastatin failed to inhibit propeptide cleavage (data not shown). In addition, we overexpressed ENPEP in several cell types and this had no effect on the kinetics of propeptide cleavage (data not shown). Furthermore, in a construct of CTHRC1 with the glutamic acid at the cleavage site changed to an alanine (E46A), cleavage still occurred indicating that ENPEP is not the protease responsible for CTHRC1 cleavage (data not shown).

In an additional experiment we investigated whether propeptide cleavage could be inhibited in a competitive and dose dependent manner by adding a synthetic peptide containing the cleavage site (Fig. 3D). As shown in Fig. 3D, >150-fold molar excess of the peptide KQKAQLRQREVVDLYNGM had no effect on the kinetics of propeptide cleavage.

3.4. Levels of full-length and cleaved CTHRC1 in circulation of healthy human subjects

We measured the levels of both full-length and total CTHRC1 in human plasma samples by ELISA to determine which forms of CTHRC1 are present in the blood of healthy subjects. As shown in Fig. 4A, the Vli10G07 ELISA was more sensitive for detection of hFL-CTHRC1 compared to the Vli42 ELISA. In addition, the Vli42 ELISA had a wider dynamic range for truncated VVD-CTHRC1 (Fig. 4B) compared to hFL-CTHRC1. Full-length CTHRC1 was detectable in 22 of the 38 subjects (58%) with levels of hFL-CTHRC1 ranging from 3.5pg/ml to 3.4ng/ml (Fig.4C), with a mean of 0.67ng/ml. Levels of total CTHRC1 were detectable in 37 of the 38 samples (97%), ranging from 88pg/ml to >400ng/ml, with a mean of 38.6ng/ml. These results show that most of the CTHRC1 present in circulation is in the form of N terminal truncated CTHRC1. Additional and larger studies are needed to determine what subject characteristics are associated with high, low or undetectable levels.

The distributions of both full-length and total CTHRC1 differ from the commonly seen bell-shaped normal distribution and instead more closely follow right-tailed exponential distributions. The maximum likelihood estimates of the exponential rate parameter for full-length and total CTHRC1 were 2.599 and 0.025, respectively. When compared to the theoretical exponential distributions with the same rates, the Pearson Goodness-of-Fit test yielded a moderate fit for the full-length CTHRC1 ($p=0.03$) and a good fit for the total CTHRC1 ($p=0.993$).

3.5. Effects of CTHRC1 on metabolism *in vitro*

Basic mechanisms of generating ATP from glucose by the cell include glycolysis and oxidative phosphorylation. The latter is more energy efficient compared to glycolysis, however, under hypoxic conditions such as in myocardial infarction, tissue damage, or tumor proliferation, an increase in glycolysis for ATP production would be beneficial. Based on our prior findings of *Cthrc1* null mice having a metabolic phenotype^{1,6} and the fact that *Cthrc1* is highly induced in response to tissue injury and in cancer stroma^{2,4}, we investigated whether CTHRC1 regulates metabolism at the cellular level. We chose primary endothelial cells, which are important players in tissue repair involving angiogenesis. We evaluated the effects of hFL-CTHRC1 containing conditioned media generated by adenoviral transduction of 3T3-L1 cells, purified recombinant hFL-CTHRC1 and purified recombinant VVD-CTHRC1 missing the propeptide (aa31–46). As shown in Fig. 5, VVD-CTHRC1 increased the basal rate of ATP production by approximately 21%, predominantly by an increase in glycolysis (Fig. 5A-C), whereas hFL-CTHRC1 was less effective. Accordingly, the percentage of ATP production from glycolysis was significantly increased, while the contribution from oxidative phosphorylation was decreased (Fig. 5D, E). Consistent with the increase in glycolysis is also the observed proportionate increase in the proton efflux rate, with VVD-CTHRC1 being more effective than hFL-CTHRC1 (Fig. 5F, G). Compensatory glycolysis in response to blocking oxidative phosphorylation was also most effectively increased in VVD-CTHRC1 treated cells (Fig. 5H). Other parameters of cell metabolism determined with the Seahorse XF Cell Mito Stress Test were not affected by CTHRC1 (supplemental data). Heat inactivation of purified VVD-CTHRC1 protein abolished its effect on glycolysis, demonstrating specificity of its effect on glycolysis

(supplemental data file Fig. 7). These findings support the notion that VVD-CTHRC1 is the most active form of CTHRC1 and that aa31–46 represent a propeptide. Although we found HUVEC not to be very efficient at propeptide cleavage compared to other cell types, it is likely that at least some of the activity of rhFL-CTHRC1 and hFL-CTHRC1 CM is attributable to ongoing generation of the VVD-CTHRC1 form while in culture. Using qRT-PCR we found transcript levels of some enzymes involved in glycolysis statistically significantly ($p < 0.02$) increased in hFL- and VVD-CTHRC1 treated cells, respectively: phosphofructokinase (1.56- and 1.46-fold), phosphoglycerate kinase (1.37- and 1.22-fold), aldolase (1.64- and 1.47-fold), and enolase (1.45- and 1.31-fold). We were unable to verify these relatively modest effects on gene expression by Western blotting. Of note, activity of glycolytic enzymes is also regulated by levels of metabolites and post-translational modifications that were not examined here ¹⁰.

3.6. Evidence for CTHRC1 promoting glycolysis in mice

We performed metabolic monitoring in wildtype and *Cthrc1* null mice with *Cthrc1* inactivation in all tissues. Mice were subjected to 24-hour activity monitoring and measurements of the respiratory exchange ratio (RER, V_{CO_2} produced/ V_{O_2} consumed) were obtained. We found that wildtype mice had significantly higher RERs over 24 hours and during the daytime compared with *Cthrc1* null mice (Fig. 6A). These data are consistent with *Cthrc1* null mice having a shift toward reduced aerobic glucose metabolism compared to wildtypes. RER is influenced by physical activity and at nighttime, when mice are active (Fig. 6D), RER values did not differ significantly between groups with an $n = 7-8$ per group (Fig. 6). At the same body weight (Fig. 6E) *Cthrc1* null mice have more fat mass and less lean mass (Fig. 6F, G). Because energy expenditure (EE) is largely determined by lean mass, we normalized EE to lean mass and this revealed no significant differences in EE between strains (Fig. 6B). During the day time when mice have very little locomotor activity, even normalization of EE to total body weight showed no significant differences between strains (Fig. 6C). A lower RER in *Cthrc1* null mice reflects decreased aerobic carbohydrate utilization, which would be consistent with effects of CTHRC1 shown in Fig. 5. Future analyses will need to determine if a reduction in RER occurs in specific tissues of *Cthrc1* null mice.

4. Discussion

We discovered CTHRC1 during a screen for novel genes induced in tissues undergoing repair in response to injury ^{2,3}. In these situations, CTHRC1 is expressed by a population of activated fibroblasts ^{3,5}. We have also shown that forced expression of CTHRC1 under *Pdgfrb* promoter control in stromal cells of transgenic mice does not contribute to CTHRC1 detectable in circulation ⁴, suggesting that CTHRC1 induced at sites of tissue injury may serve functions associated with localized tissue repair. Tissue repair and remodeling are also part of expanding solid tumors where CTHRC1 is expressed by the cancer activated fibroblast (supplemental data Fig. 9) ⁴. Tissue injury is accompanied by damage to blood vessels and interruption of blood supply, leading to hypoxia and inability to meet the metabolic needs of the tissue. In mice, expression of CTHRC1 occurs within 3 days of injury in activated fibroblasts ³. We expect that during tissue injury blood clotting

occurs with activation of proteases present in serum, in addition to release of intracellular factors from damaged cells. As shown here, both serum and intracellular components contributed to propeptide cleavage of CTHRC1 that could be partially inhibited by a combination of protease inhibitors (Fig. 2, 3). Although we were not able to identify a specific protease or class of proteases responsible for propeptide cleavage, we anticipate that the requirements for CTHRC1 activation at sites of tissue injury are met based on our findings. We envision that activated CTHRC1 will increase glycolytic metabolism of endothelial cells at the site of injury, which in turn is expected to facilitate angiogenesis in the hypoxic environment in which ATP production via mitochondrial respiration is limited. In addition, ATP production via glycolysis is >10-fold faster compared to generation by cell respiration, further facilitating wound healing. In the present study we did not conduct *in vivo* angiogenesis experiments, which need to be carried out in the future to verify the concept of CTHRC1 function proposed here. Future experiments also need to address the mechanisms by which glycolysis is promoted by CTHRC1 with potential regulation of activities of glycolytic enzymes and whether the observed effects are directly or indirectly mediated by CTHRC1. In addition, an important and clinically relevant question would also be whether exogenous CTHRC1 has therapeutic potential in the treatment of chronic wounds.

The successful production and purification of recombinant CTHRC1 has previously been a challenge as aggregation of the protein presented a major obstacle for functional studies. Several publications report on diverse effects of purified CTHRC1 often used at unphysiological concentrations (for review ¹¹), although a robust readout for CTHRC1 activity has hitherto remained elusive in our hands.

With development of monoclonal antibodies for detection of CTHRC1 by ELISA we have been able to show, i) that the N terminal 16 amino acids following the signal peptide represent a propeptide that requires cleavage for increased biological activity, ii) that active CTHRC1 is the most abundant form of CTHRC1 in human plasma, and iii) that the concentrations of CTHRC1 in plasma in healthy subjects range from undetectable to >400ng/ml following an exponential distribution. Using purified recombinant CTHRC1 at physiological concentrations we demonstrate that CTHRC1 robustly promotes glycolytic metabolism in endothelial cells, which presents a novel and reliable readout for CTHRC1 activity. CTHRC1 had no effect on endothelial cell proliferation (supplemental data file). Cleaved VVD-CTHRC1 was found to be the most active form in these assays, which is consistent with the N terminus encoding a propeptide. However, we were not able to determine whether hFL-CTHRC1 is simply less active versus not active at all because in the presence of cells, cleavage of the propeptide occurs over time, although many cell types tested were more efficient than HUVECs in converting hFL-CTHRC1 to VVD-CTHRC1. Using respirometry and metabolic monitoring in wildtype and global *Cthrc1* null mice we were able to corroborate that CTHRC1 promotes glycolysis *in vivo* by detecting a higher RER in wildtype mice compared to *Cthrc1* nulls. Although CTHRC1 is produced in bone of rodents ⁵, unlike humans, circulating levels in mice are usually below the level of detection (data not shown). This raises questions about the significance and role of CTHRC1 in human plasma. With most of it in the VVD-CTHRC1 form there is the possibility that this pool is readily available to interact with putative receptor(s) to exert its biological effects. Future

studies could determine whether an association between RER and plasma CTHRC1 levels exists in humans, and whether the relative ratios of hFL- and VVD-CTHRC1 are linked to physiology and/or pathology.

CTHRC1 has been most extensively published on in the context of cancer, with many studies erroneously reporting overexpression of CTHRC1 in cancer cells themselves. With monoclonal antibodies validated on *Cthrc1* null tissues we demonstrated that most of the CTHRC1 in tumors is expressed by the stromal cells associated with the tumor, the cancer activated fibroblast (supplemental data Fig. 9) ⁴. High levels of CTHRC1 expression in cancers have been associated with increased invasiveness and poor outcome ¹¹. While experiments here focused on endothelial cells not cancer, there is the possibility that our findings are relevant to solid tumors as well. Tumors are often hypoxic and CTHRC1 expressed by CAFs could facilitate angiogenesis by promoting glycolysis in endothelial cells, thereby promoting tumor growth. Of note is that CTHRC1 increases glycolysis under normoxic conditions, which brings to mind the Warburg effect (for review ¹²), characteristically observed in many cancer cells with highly glycolytic metabolism occurring in the absence of hypoxic conditions, a phenomenon termed aerobic glycolysis. The causes and function of the Warburg effect are still unclear despite thousands of publications just within the last few years. We acknowledge that translation of the results of this study to cancer is speculative as we do not address the role of CTHRC1 in cancer. Support for the hypothesis that CTHRC1 is a candidate contributing mediator of the Warburg effect is, however, consistent with the data shown in Fig. 5, as VVD-CTHRC1 caused a 20.9% increase in total basal ATP production with a 33.3% increase in basal ATP production from glycolysis under standard tissue culture conditions. Obvious questions related to this are whether CTHRC1 produced by adjacent CAFs is causing the shift toward glycolysis or whether circulating levels of CTHRC1 or both contribute to the Warburg effect if a putative CTHRC1 receptor is expressed on the tumor cell. Furthermore, it is widely accepted that glycolysis also occurs under normoxic conditions *in vivo* (for review ¹³).

In summary, our studies provide novel insight into activation of CTHRC1, its biological activity in promoting glycolysis with potential implications for angiogenesis including tumor angiogenesis, and CTHRC1 plasma levels in humans. Furthermore, our data provide rationales for future experiments related to angiogenesis and tumor cell metabolism.

Supplementary Material

Refer to Web version on PubMed Central for supplementary material.

Acknowledgements

This work was supported by NIH grant HL146504 and utilized services of the Physiology Core, Histopathology Core, Confocal Microscopy Core, and Mouse Transgenic Core which are supported by NIH/NIGMS P30GM106391 and P20GM121301. Project support was also provided by funds from the MaineHealth Institute for Research.

6. References

1. Stohn JP, Perreault NG, Wang Q, Liaw L, Lindner V. Cthrc1, a novel circulating hormone regulating metabolism. *PLoS One*. 2012;7:e47142. doi: 10.1371/journal.pone.0047142 [PubMed: 23056600]
2. Pyagay P, Heroult M, Wang Q, Lehnert W, Belden J, Liaw L, Friesel RE, Lindner V. Collagen triple helix repeat containing 1, a novel secreted protein in injured and diseased arteries, inhibits collagen expression and promotes cell migration. *Circ Res*. 2005;96:261–268. doi: 10.1161/01.RES.0000154262.07264.12 [PubMed: 15618538]
3. Ruiz-Villalba A, Romero JP, Hernandez SC, Vilas-Zornoza A, Fortelny N, Castro-Labrador L, San Martin-Uriz P, Lorenzo-Vivas E, Garcia-Olloqui P, Palacio M, et al. Single-Cell RNA Sequencing Analysis Reveals a Crucial Role for CTHRC1 (Collagen Triple Helix Repeat Containing 1) Cardiac Fibroblasts After Myocardial Infarction. *Circulation*. 2020;142:1831–1847. doi: 10.1161/CIRCULATIONAHA.119.044557 [PubMed: 32972203]
4. Duarte CW, Stohn JP, Wang Q, Emery IF, Prueser A, Lindner V. Elevated plasma levels of the pituitary hormone Cthrc1 in individuals with red hair but not in patients with solid tumors. *PLoS One*. 2014;9:e100449. doi: 10.1371/journal.pone.0100449 [PubMed: 24945147]
5. Jin YR, Stohn JP, Wang Q, Nagano K, Baron R, Bouxsein ML, Rosen CJ, Adarichev VA, Lindner V. Inhibition of osteoclast differentiation and collagen antibody-induced arthritis by CTHRC1. *Bone*. 2017;97:153–167. doi: 10.1016/j.bone.2017.01.022 [PubMed: 28115279]
6. Stohn JP, Wang Q, Siviski ME, Kennedy K, Jin YR, Kacer D, DeMambro V, Liaw L, Vary CP, Rosen CJ, et al. Cthrc1 controls adipose tissue formation, body composition, and physical activity. *Obesity (Silver Spring)*. 2015;23:1633–1642. doi: 10.1002/oby.21144 [PubMed: 26148471]
7. Myngbay A, Bexeitov Y, Adilbayeva A, Assylbekov Z, Yevstratenko BP, Aitzhanova RM, Matkarimov B, Adarichev VA, Kunz J. CTHRC1: A New Candidate Biomarker for Improved Rheumatoid Arthritis Diagnosis. *Front Immunol*. 2019;10:1353. doi: 10.3389/fimmu.2019.01353 [PubMed: 31249576]
8. Shekhani MT, Forde TS, Adilbayeva A, Ramez M, Myngbay A, Bexeitov Y, Lindner V, Adarichev VA. Collagen triple helix repeat containing 1 is a new promigratory marker of arthritic pannus. *Arthritis Res Ther*. 2016;18:171. doi: 10.1186/s13075-016-1067-1 [PubMed: 27430622]
9. Leclair RJ, Wang Q, Benson MA, Prudovsky I, Lindner V. Intracellular localization of Cthrc1 characterizes differentiated smooth muscle. *Arterioscler Thromb Vasc Biol*. 2008;28:1332–1338. doi: 10.1161/ATVBAHA.108.166579 [PubMed: 18467647]
10. Hagopian K, Tomilov AA, Kim K, Cortopassi GA, Ramsey JJ. Key glycolytic enzyme activities of skeletal muscle are decreased under fed and fasted states in mice with knocked down levels of Shc proteins. *PLoS One*. 2015;10:e0124204. doi: 10.1371/journal.pone.0124204 [PubMed: 25880638]
11. Mei D, Zhu Y, Zhang L, Wei W. The Role of CTHRC1 in Regulation of Multiple Signaling and Tumor Progression and Metastasis. *Mediators Inflamm*. 2020;2020:9578701. doi: 10.1155/2020/9578701 [PubMed: 32848510]
12. Vaupel P, Multhoff G. Revisiting the Warburg effect: historical dogma versus current understanding. *J Physiol*. 2021;599:1745–1757. doi: 10.1113/JP278810 [PubMed: 33347611]
13. Brooks GA. The Science and Translation of Lactate Shuttle Theory. *Cell Metab*. 2018;27:757–785. doi: 10.1016/j.cmet.2018.03.008 [PubMed: 29617642]

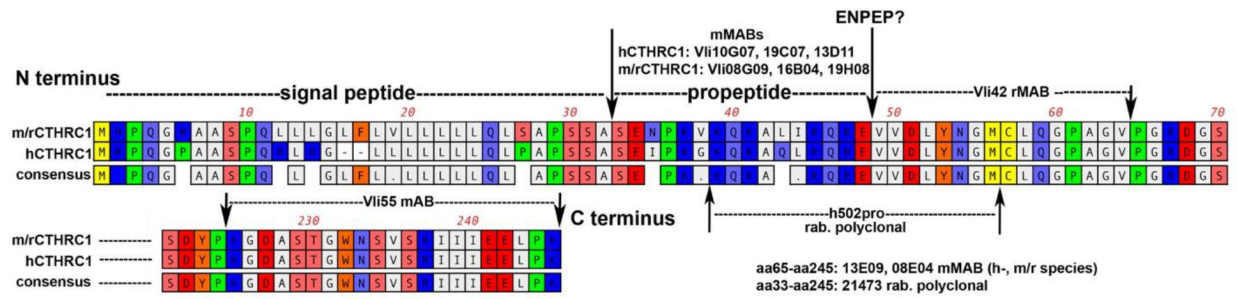
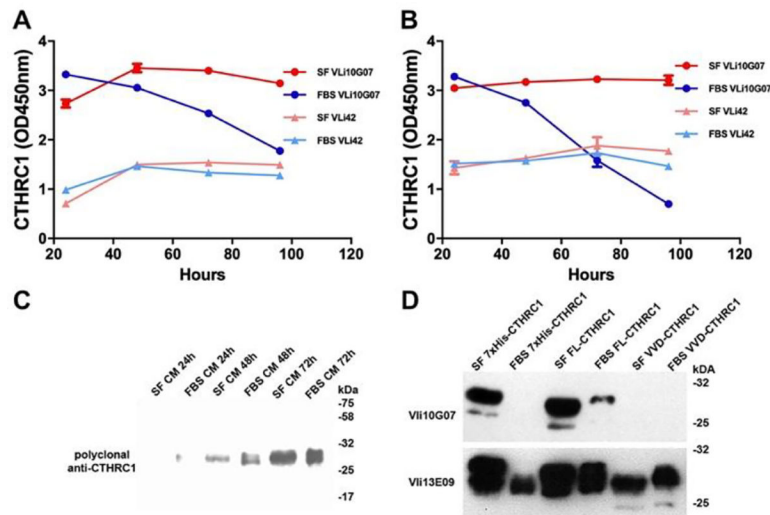


Figure 1. A schematic of the epitopes within the CTHRC1 protein sequence recognized by the antibodies generated is shown. h=human, m=mouse, r=rat, rab=rabbit, MAB=monoclonal antibody.

**Figure 2.**

Cleavage of CTHRC1 by CHOK1 and HEK293T cells transfected with human full-length CTHRC1 over time was monitored by ELISA and Western blotting. Over the course of 4 days the levels of full-length CTHRC1 decline in samples containing serum (FBS) in CHOK1 cells (A) and HEK293T cells (B), while total levels of CTHRC1 determined with Vli42 plateau at 48 hours. In the absence of serum, levels of full-length CTHRC1 show little to no reduction over 4 days. The graphs are representative of more than 10 separate experiments. (C) CTHRC1 levels in CM in the presence (FBS) and absence (SF) of serum over time are shown by immunoblotting with a polyclonal antibody recognizing full-length and N terminally truncated CTHRC1. In the presence of serum, a band of lower molecular weight is apparent within 48 hours. (D) HEK293T cells were transfected with different constructs of CTHRC1 and CM were analyzed by immunoblotting 72h later. Samples were probed with monoclonal antibodies that recognize the full-length form of CTHRC1 (Vli10G07) or all forms of CTHRC1 (Vli13E09).

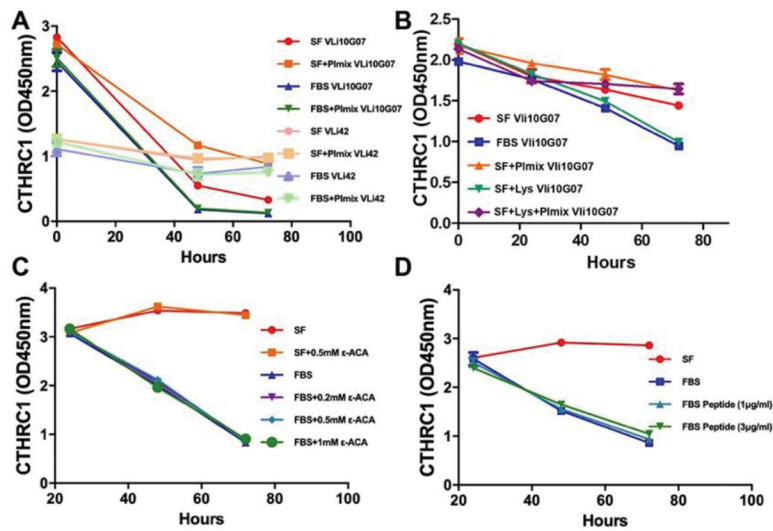


Figure 3.

Propeptide cleavage is partially blocked by protease inhibitors. (A) hFL-CTHRC1 CM was added to HEK293T in the presence (FBS) or absence (SF) of serum, with or without addition of protease inhibitor cocktail (Pimix). Full-length CTHRC1 was detected with Vli10G07 and cleaved CTHRC1 with Vli42. (B) hFL-CTHRC1 CM was incubated with or without lysate from HEK293T cells (Lys) added under conditions as indicated. (C) Propeptide cleavage was neither inhibited by ϵ -aminocaproic acid (ϵ -ACA), (D) nor by addition of a synthetic peptide containing the cleavage site. All experiments were carried out in replicates of >3 with similar results.

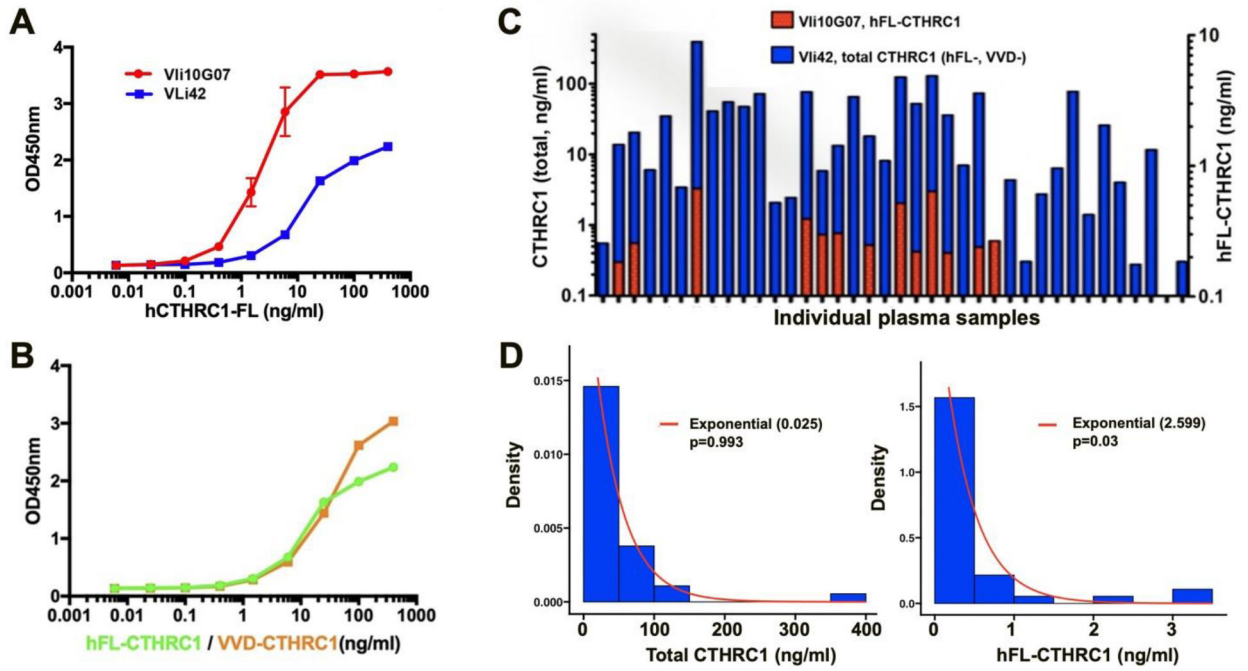


Figure 4.

Standard curves for ELISAs detecting only hFL-CTHRC1 (Vli10G07) or both hFL- and VVD-CTHRC1 (Vli42) are shown along with their respective plasma levels in healthy human subjects. (A) Vli10G07 is more sensitive for detection of hFL-CTHRC1 compared to Vli42. (B) Vli42 has a wider dynamic range for detection of VVD- versus hFL-CTHRC1. (C) Plasma levels of total CTHRC1 (in blue) with the fraction of hFL-CTHRC1 (in red) in human plasma samples are shown for each subject. Levels of hFL-CTHRC1 were detectable in 58% of the samples tested. Note that the scale of the y-axes differs by a factor of more than 10, demonstrating that most of the CTHRC1 in circulation is of the cleaved form. (D) Distribution of total CTHRC1 and hFL-CTHRC1 with corresponding theoretical exponential probability density functions in red. The Pearson Goodness-of-Fit test of no difference between the distributions showed a moderate fit ($p=0.03$) for hFL-CTHRC1 and a good fit ($p=0.993$) for total CTHRC1. Bins for testing hFL-CTHRC1 were 0–0.5, 0.5–1, 1–1.5, and >1.5. Bins for testing total CTHRC1 were 0–50, 50–100, 100–150, and >150.

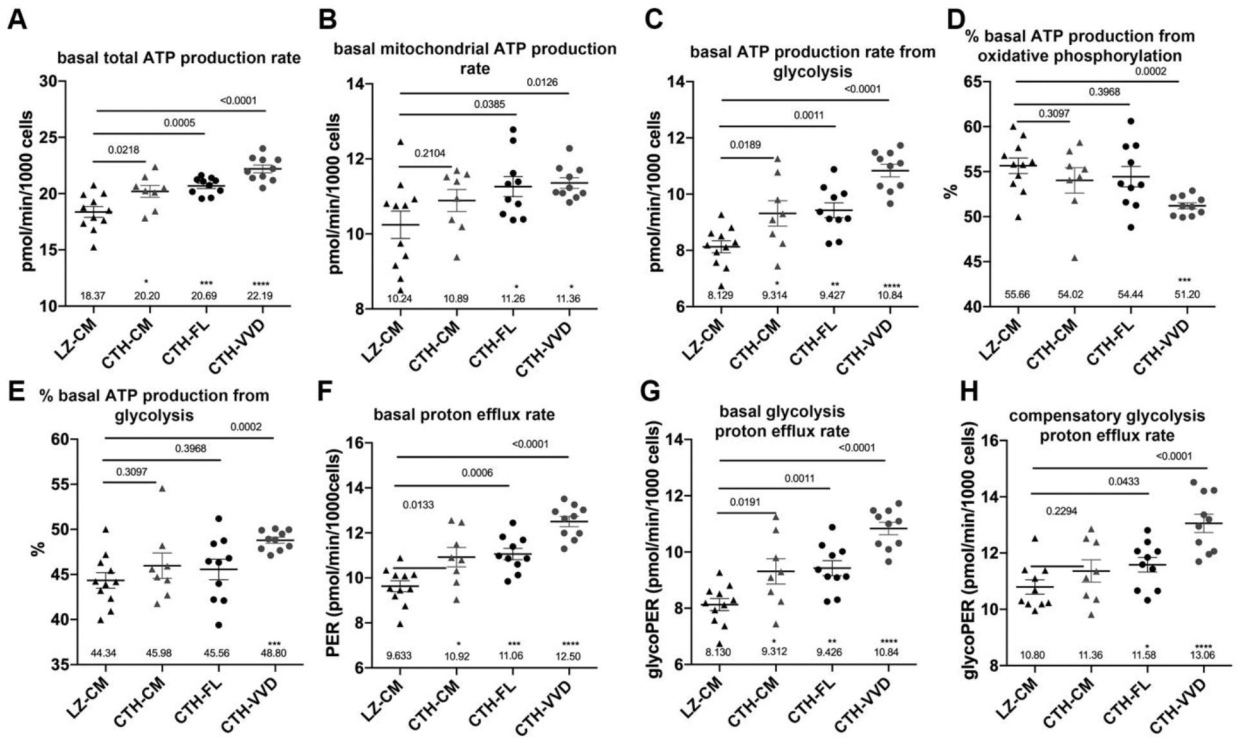


Figure 5. Increase in glycolysis by CTHRC1 in HUVEC as investigated by Seahorse technology is shown. Recombinant cleaved CTHRC1 (rhVVD-CTHRC1, CTH-VVD) increases glycolysis in endothelial cells whereas recombinant full-length CTHRC1 (rhFL-CTHRC1, CTH-FL) and full-length CTHRC1 conditioned medium from transduced cells (hFL-CTHRC1 CM, CTH-CM) are less or not active compared to control medium (LZ-CM). Representative results of three independent experiments of cell metabolic analyses using Seahorse technology are shown. Both recombinant proteins were used at 200ng/ml, which is a physiologically relevant concentration based on human plasma levels shown in Fig. 4C. PER = proton efflux rate, mean \pm SEM and p values were calculated with unpaired Student's t-test.

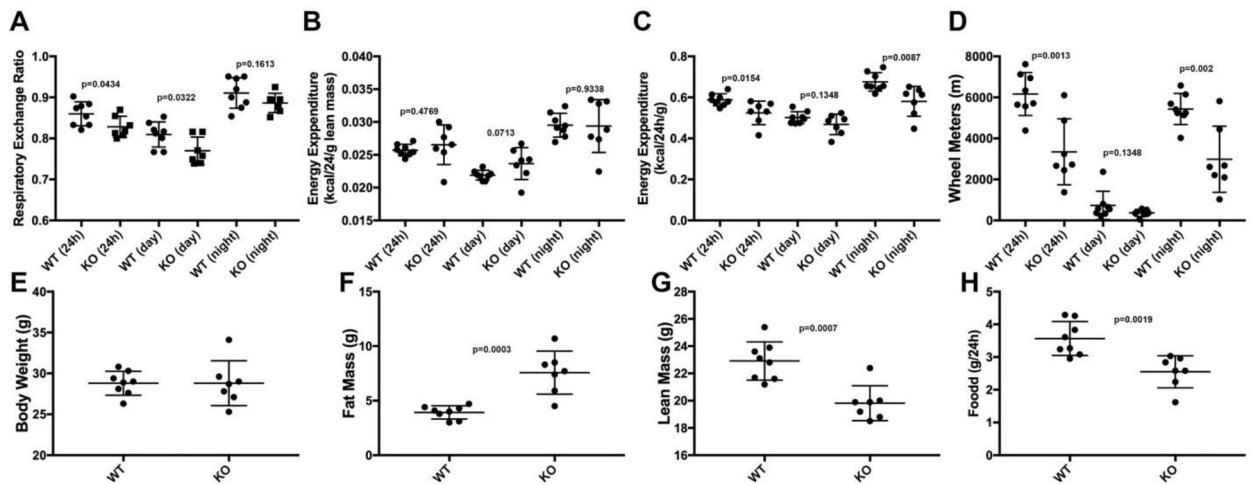


Figure 6.

(A) Wildtype mice (WT) have a higher average respiratory exchange ratio (RER) during the daytime and over a 24-hour period compared to *Cthrc1* null mice (KO) as determined by metabolic monitoring. RER at night when mice are active (D, running wheel distance) and energy expenditure normalized to lean mass (B), as well as body weight (E) were not significantly different between strains. Whole body composition as determined by NMR (F, G) differs between strains with KO mice having more fat mass at the expense of a proportionate reduction in lean mass. Data collected for separate day time and night time readouts were projected for a 24-hour period to facilitate comparison (B, C). Mean \pm SEM and p values calculated with Student's t test are shown.